Microscopic Examination of Free-Energy Relationships for Electron Transfer in Polar Solvents

Jenn-Kang Hwang and Arieh Warshel*

Contribution from the Department of Chemistry, University of Southern California, Los Angeles, California 90089-0482. *Received August 22, 1986*

Abstract: A recently developed semiclassical trajectory (ST) approach is used to explore the microscopic free-energy relationship for electron-transfer reactions in polar solvents. The free-energy functional is evaluated by an adiabatic charging process based on the umbrella sampling method. The relevant energy fluctuations are generated by molecular dynamics simulation, representing the solvent molecules by the surface constrained all atom solvent (SCAAS) model. The specific model considered is composed of two benzene-like molecules with variable redox potentials. The simulation gives stable results with a relatively small convergence error. The results are compared to the free-energy profile predicted by the macroscopic Marcus' model. It is found that the solvent contribution to the activation barrier follows Marcus' relationship, provided that the reorganization energy parameter is evaluated from the microscopic simulation. The experimentally observed deviations from Marcus' relationship are shown, by realistic microscopic calculations, to be due to the solute vibronic channels. It is pointed out that the approximately quadratic behavior of the free-energy functional might reflect an inherent property of solvents with high dielectric constant.

I. Introduction

Electron-transfer (ET) reactions play a major role in many chemical and biological processes. Extensive studies of this class of reaction (see, for example, ref 1–12) have identified key factors and provide a qualitative and sometimes quantitative understanding of the relation between the rate constants and the nature of the reacting systems. The rate constant can be expressed as

$$k \simeq \sigma^2(\mathbf{R}) \exp[-\Delta g^{\ddagger}(\alpha_i,\alpha_s,\Delta G_0,\mathbf{R})/k_B T] \quad (1)$$

where k_B is the Boltzmann constant, and R is the distance between the donor and acceptor. The key factors in ET reactions are the following: (i) the coupling term between the donor and acceptor, $\sigma(\mathbf{R})$; (ii) the free-energy difference between the products and reactants, ΔG_0; (iii) the reorganization energy, α_s, of the solvent around the donor and acceptor; (iv) the intramolecular reorganization energy, α_i, in the donor and acceptor. The search for the relationship between the parameters $\mathbf{R}$, ΔG_0, α_i, and α_s and the activation free energy for ET reactions, $\Delta g^{\ddagger}$, has been the objective of many studies of ET reactions. The basic theoretical guideline for this search was developed by Marcus[1] and Levich[2] and later extended by others. The key role of the solvent and the importance of using free energy rather than potential energy was recognized by Marcus who gave (for structureless donor and acceptor, held at a fixed distance in a dielectric continuum) the relation

$$\Delta g^{\ddagger} = (\alpha_s + \Delta G_0)^2/4\alpha_s \quad (2)$$

where α_s is the solvent reorganization energy. The effect on $\Delta g^{\ddagger}$ by the molecular vibrations of the donor and acceptor was formally incorporated in quantum mechanical and semiclassical treatments (see, for example, ref 3c and 8).

In the past few years we have witnessed a very intense experimental effort in studying ET reactions (see, for example, ref 9–12). This impressive effort has started to push the field from the qualitative range to the quantitative direction. Model compounds have been built with fixed distances between donors and acceptors, thus isolating the effect of $\mathbf{R}$ on the rate constant. Changing solvents and ΔG_0 for fixed $\mathbf{R}$ started to give more quantitative information about the exact role of α and ΔG_0. Ultrafast time-resolved experiments have started to give exciting results about the relation between the rate constant and the dynamics of the surrounding solvents. The recent experiments appear to confirm, in a qualitative way, the available theories. However, on the detailed quantitative level one still faces major open questions. One of the most fundamental questions is concerned with the validity of eq 2 on the microscopic level. This equation is based on the continuum description of the solvent, which is the basis of most electrostatic theories. Yet the solvent polarization by nearby charges might not follow the macroscopic assumptions. In fact, eq 2 is recovered if one describes the solvent in the harmonic approximation[14] and therefore cannot be exact for highly anharmonic systems.

Experimental attempts to explore the range of validity of Marcus' relationship (eq 2) have moved a long way and gave encouraging results. However, at present it appears that the available experimental approaches cannot provide an accurate estimate of the contribution of the solvent to $\Delta g^{\ddagger}$. That is, the impressive study of Miller and co-workers[9] presented a fit of the calculated and observed dependence of the rate constant on ΔG_0 by using three adjustable parameters (solvent reorganization energy, solute reorganization energy, and an effective vibrational frequency). Such a fit cannot be used to elucidate the exact nature of $\Delta g^{\ddagger}$. In order to examine a theoretical expression one needs to evaluate the relevant parameters from independent experiments or theory. Apparently, it is hard to determine quantitatively the value of the solvent reorganization energy for different donors and acceptors.[27] Similarly it is not simple to obtain the solute reorganization energies (Franck–Condon factors) and extracting such parameters by fitting the calculated and observed rate constants does not constitute a unique examination of the given rate expression.

In view of the above difficulties, it seems useful to consider computer simulation approaches as alternative and complementary ways of examining the microscopic nature of $\Delta g^{\ddagger}$. This is done in the present work which uses a semiclassical trajectory approach

(1) (a) Marcus, R. A. *J. Chem. Phys.* **1956**, *24*, 966. (b) Marcus, R. A. *Ibid.* **1956**, *24*, 979. (c) Marcus, R. A. *Annu. Rev. Phys. Chem.* **1964**, *15*, 155.
(2) Levich, V. G. *Adv. Electrochem. Electrochem. Eng.* **1966**, *4*, 249.
(3) (a) Hopfield, J. J. *Proc. Natl. Acad. Sci. U.S.A.* **1974**, *71*, 3640. (b) Jortner, J. *J. Chem. Phys.* **1976**, *64*, 4860. (c) Efirma, S.; Bixon, M. *J. Chem. Phys.* **1976**, *64*, 3639. (d) Bixon, M.; Jortner, J. *Faraday Discuss. Chem. Soc.* **1982**, *74*, 17.
(4) Dogonadze, R. R.; Kuznetsov, A. M. *Elektrokhimiya* **1967**, *3*, 1324. Dogonadze, R. R.; Kuznetsov, A. M. *Sov. Electrochem. Engl. Transl.* **1967**, *3*, 1189.
(5) (a) Ulstrup, J. *Charge Transfer Processes in Condensed Media*; Springer-Verlag: Berlin, 1979. (b) Devault, D. *Quart. Rev. Biophys.* **1980**, *13*, 387. (c) Newton, M. D.; Sutin, N. *Annu. Rev. Phys. Chem.* **1984**, *35*, 437.
(6) (a) Huppert, D.; Kanety, H.; Kosower, E. M. *Faraday Discuss. Chem. Soc.* **1982**, *74*, 161. (b) Kosower, E. M. *J. Am. Chem. Soc.* **1985**, *107*, 1114.
(7) Churg, A. K.; Weiss, R. M.; Warshel, A.; Takano, T. *J. Phys. Chem.* **1983**, *87*, 1683.
(8) Warshel, A. *J. Phys. Chem.* **1982**, *86*, 2218.
(9) (a) Miller, J. R.; Beitz, J. V.; Huddleston, R. K. *J. Am. Chem. Soc.* **1984**, *106*, 5057. (b) Miller, J. R.; Calcaterra, L. T.; Closs, G. L. *J. Am. Chem. Soc.* **1984**, *106*, 3047.

0002-7863/87/1509-0715$01.50/0

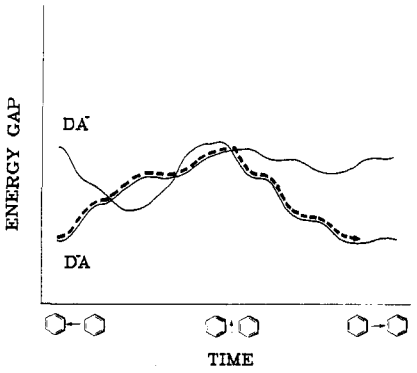

Figure 1. A schematic description of an electron-transfer reaction between two benzene type molecules. The reaction coordinate is represented by the orientation of a single dipole. The reaction is basically a surface crossing process between the D^-A surface and the DA^- surface; whenever $\Delta\epsilon = 0$ the trajectory can cross from the reactant state to the product state.

in exploring the validity of eq 2 on a microscopic level.

Our study evaluates the actual activation free energy of ET reactions for a model system of two benzene molecules in water. It is found that eq 2 does provide a good description of the actual microscopic results. This is obtained, however, only if α is evaluated by microscopic calculations, which can be quite different from the corresponding macroscopic estimates. It is also found that the deviations from eq 2 at the inverted region (where $|\Delta G_0| > \alpha$) can be accounted for by considering the solute vibronic channels.

II. Simulating ET Processes in Polar Solvents by the Semiclassical Trajectory Approach

As indicated by Figure 1, one can consider an ET reaction as a crossing between two electronic surfaces (for more discussion see ref 14). This surface crossing process is induced by fluctuation of the solvent dipoles, and the transition occurs at points where the two surfaces intersect. To simulate the effect of the solvent fluctuations on the ET process, we use the following semiclassical model.

The reactant and product are considered as two zero-order electronic states ϕ_a and ϕ_b, and thus the complete system is described by the time-dependent wavefunctions

$$\psi = C_a\phi_a(\mathbf{r}) \exp\left\{-(i/\hbar)\int^t dt'\epsilon_a(t')\right\} + C_b\phi_b(\mathbf{r}) \exp\left\{-(i/\hbar)\int^t dt'\epsilon_b(t')\right\} \quad (3)$$

where $\mathbf{r}$ describes the solvent coordinates and $V_\alpha(\mathbf{r})$ is the solute + solvent potential surface in the αth electronic state. Substituting this equation into the time dependent Schrodinger equation, we get

$$C_a(\tau) = \int_0^\tau \dot{C}_a(t)\,dt = \int_0^\tau -(i/\hbar)\sigma \exp\left\{(i/\hbar)\int_0^t dt'\Delta\epsilon_{ab}(\mathbf{r}(t'))\right\}C_b(t)\,dt$$

$$C_b(\tau) = \int_0^\tau \dot{C}_b(t)\,dt = \int_0^\tau -(i/\hbar)\sigma \exp\left\{(i/\hbar)\int_0^t dt'\Delta\epsilon_{ba}(\mathbf{r}(t'))\right\}C_a(t)\,dt \quad (4)$$

where $\Delta\epsilon_{ba} = \epsilon_b - \epsilon_a$, σ is $\langle\phi_a|H|\phi_b\rangle$, and where we use the initial condition $C_a(0) = 1$, $C_b(0) = 0$. $C_b^2(t)$ is the probability of being in state b at the time t. The above expression corresponds to the diabatic limit where σ is sufficiently small so that eq 4 can be integrated in a stable way ($C_a(t)$ stays close to one). When σ is large we switch to the adiabatic representation.[14]

The rate constant for the transition from the reactant to the product state is determined by evaluating the probability of being at state b (C_b^2). This is done by propagating trajectories of the solvent molecules according to the classical Hamilton equations

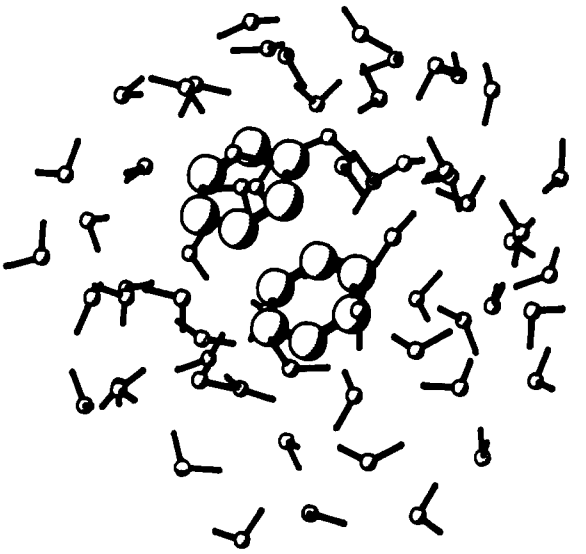

Figure 2. Showing snapshot of one of the many spacial configurations generated by molecular dynamics simulation of an SCAAS model consists of two benzene molecules separated by 5 Å and 60 water molecules.

of the system and evaluating the energy gap $\Delta\epsilon(\mathbf{r}(t))$ along the trajectories (Figure 3). The rate constant, k, is then calculated by using the following equation

$$k = \left\langle (1/\tau)\left|\int_0^\tau C_b(t)\,dt\right|^2\right\rangle_0 \quad (5)$$

where $\langle\ \rangle_0$ indicates an average over initial conditions which is *automatically* obtained by integrating a long time trajectory in a many dimensional system.

Our approach, which was introduced in a somewhat ad hoc way,[8] appears now to be quite rigorous. That is, this approach (that does not reproduce the quantum mechanical rate constant at the low-temperature limit[14]) converges to the exact quantum mechanical result for the harmonic test case at the high-temperature limit. More importantly, in treating anharmonic systems at the statistical limit we obtain[8,14]

$$k = (\sigma/\hbar)^2(\pi\hbar^2/k_BT\alpha)^{1/2} \exp(-\Delta g^*\beta) \quad (6)$$

where k_B is the Boltzmann constant, $\beta = 1/k_BT$, and Δg^* is the activation free energy associated with the probability of reaching the transition state. This important point can be best understood by considering the fact that integration of C_b (eq 4) gives significant contributions only when the energy gap $\Delta\epsilon(t)$ approaches zero. Thus we basically evaluate (see Figure 1) the number of times the system reaches points with zero energy gap weighted by the average probability of surface crossing (the Landau–Zener probability). The number of times of reaching the points in phase space with $\Delta\epsilon = 0$ is directly related to the probability (and the corresponding free energy) associated with this region. Equation 5 provides a simple yet reliable way for computer simulation of electron-transfer reactions in solutions.

Here we choose as a model system two benzene molecules in water. This system can be used as a model for electron transfer between aromatic molecules by adjusting the oxidation and redox potentials of the donor and acceptor. The dynamics of the solute + solvent system is simulated by the surface constrained all-arom solvent (SCAAS) model. This model represents the solute and

(10) Yocom, K. M.; Shelton, J. B.; Shelton, J. R.; Schroeder, W. A.; Worosila, G.; Isied, S. S.; Bordignon, E.; Gray, H. B. *Proc. Natl. Acad. Sci. U.S.A.* **1982**, *79*, 7052.
(11) Wasielewski, M. R.; Niemczyk, M. P.; Svec, W. A.; Pewitt, E. B. *J. Am. Chem. Soc.* **1985**, *107*, 1080.
(12) Isied, S. S.; Worosila, G.; Atherton, S. J. *J. Am. Chem. Soc.* **1982**, *104*, 7659.
(13) Churg, A. K.; Warshel, A. In *Structure and Motion: Membranes, Nucleic Acid and Proteins*; Clementi, E., Corongiu, G., Sarma, M. H., Sarma, R. H., Eds.; Adenine Press: New York, 1985; p 361.
(14) Warshel, A.; Hwang, J.-K. *J. Chem. Phys.* **1986**, *84*, 4938.

Table I. Parameters Used in Calculations[a]

type	parameter	value
water charge	Q_O	−0.8
	Q_H	0.4
van der Waals	A_{OO},B_{OO}	629000, −625
	A_{CO},B_{CO}	450000, −600

[a] A and B are the coefficients of the r^{-12} and r^{-6} terms, in units of Å^{12} kcal/mol and Å^6 kcal/mol, respectively. The van der Waals interactions involving the water hydrogens are taken as zero. Charges are given in units of electron charge.

the first few solvation shells by all atom model of the solute and water molecules. The boundary conditions are introduced by surrounding the system by a surface of water molecules which are subjected to constraint forces as well as the internal forces of the systems. The constraint forces are introduced in order to force the average polarization, radial distances, and the average fluctuations of the surface molecules to be close to those expected from the corresponding infinite system. The specific calculations described in this work were done by holding the two benzene molecules 5 Å apart in an environment of 60 water molecules. A typical snapshot generated by the simulation is described in Figure 2. The parameters used in the simulation are given in Table I.

The direct evaluation of eq 5 is particularly useful for studying fast ET reactions, which can be simulated by investing a reasonable computer time. For example, we present in Figure 3 a direct simulation of a case where the energy difference between the product and reactant states is taken as −40 kcal/mol. This selection leads to a small activation barrier, and the two surface intersect frequently during the simulation time. As shown from Figure 3, the probability C_b^2 increases significantly only when the surfaces intersect, thus the rate constant is basically the average of the contributions from the different crossing processes. The direct simulation approach is particularly powerful in exploring dynamical effects associated with the solvent dielectric relaxation.[14] Such studies (which will be reported elsewhere) are not the subject of the present work; our main subject is the evaluation of activation energies, which will be considered next.

III. Evaluating Activation Free Energies by an Adiabatic Charging Process

Obtaining a rate expression which is related to free energy rather than potential energy is a key point of our semiclassical approach. Yet, eq 5 cannot be evaluated directly for cases with high activation barrier, since it takes on extremely long computer time to reach points where the two surface intersect. Thus one has to evaluate the average number of time the system reaches the transition state by an indirect method. To do this we consider the statistical probability that the system will be at the region X^* in phase space where $\Delta\epsilon = 0$. The relevant probability factor $P(X^*)$ is in fact (see ref 14) the factor $\exp(-\Delta g^*\beta)$ in eq 6, whose evaluation is the primary objective of this work.

Our evaluation of $P(X^*)$ is based on a "charging" method that utilizes the umbrella sampling technique.[20,8] This approach (which was introduced in a preliminary way in ref 8) is described below by using the specific simulation for clarification.

As argued above, one would like to evaluate the probability that an infinitively long trajectory on the reactant surfaces will reach the hypersurface where the reactant and product surfaces intersect. To evaluate this probability we divide the total partition function of the system into partial partition functions that correspond to the yet to be defined reaction coordinate

$$\mathbf{q}_G(X_m) = \int \exp\{-E_G(X_m,\mathbf{S})\beta\}\, d\mathbf{S} \qquad (7)$$

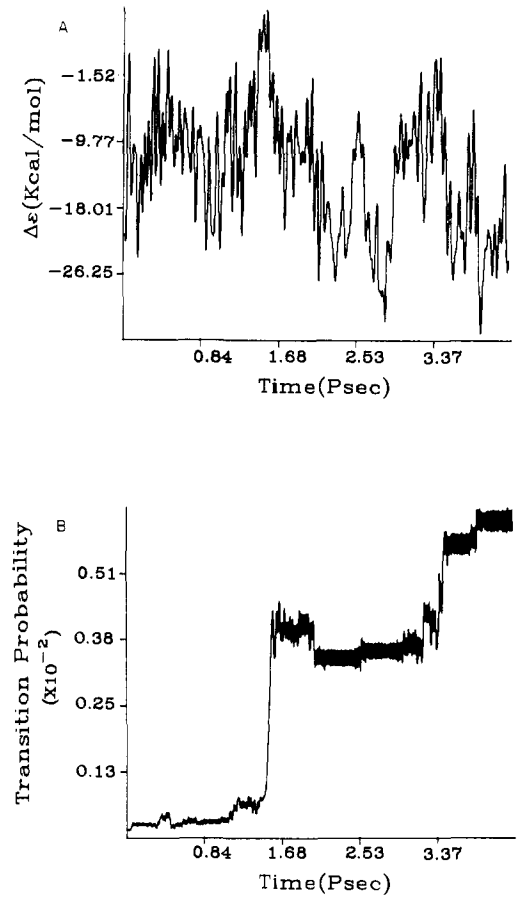

Figure 3. The relation between the reaction probability and the time dependent energy gap. The figure describes the energy gap for our model system and the corresponding probability C_b^2.

where $\mathbf{S}$ is the subset of coordinates in the configuration space with the particular value of X_m, and E_G is the ground-state potential surface. Taking the partial partition function $\mathbf{q}_G(X_a)$ at the most probable value of $X = X_a$ in the reactant region as a reference, we define $P(X)$ in terms of the relative partition function $q_G(X_m) = \mathbf{q}_G(X_m)/\mathbf{q}_G(X_a)$ by

$$P(X_m)\Delta X = \int_{X_m}^{X_m+\Delta X} q_G(X)\, dX/Q_a \qquad (8)$$

where

$$Q_a = \int_{-\infty}^{X^*} q_G(X)\, dX \qquad (9)$$

In principle one can evaluate eq 8 by running trajectories and finding the ratio between the time spent at the region ($X_m > X > X_m + \Delta X$) and the total trajectory time. This direct approach is, however, not practical in cases of significant activation barriers. In such cases it might take an enormous amount of time for a trajectory that started at the reactant region to reach the product region. This problem can be overcome by finding a sampling potential, ϵ_m, that forces the trajectory to spend most of its time near X_m and relating the probability of being at X_m to the free energy associated with changing E_G to ϵ_m. The relevant procedure can be best understood by considering it in several steps, first the evaluation of the free energy associated with the change of the potential of the system, second the selection of an effective mapping potential and finally the evaluation of the relevant $q_G(X_m)$.

The free energy associated with changing the potential of the system from the real potential E_G to the sampling potential ϵ_m is evaluated by the umbrella sampling method,[20] considering the ratio between the corresponding partition functions

$$\exp(-\Delta G_{G\to m}\beta) = Q_m/Q_G = \int\int \exp\{-\epsilon_m\beta\}\, d\mathbf{S}\, dX/Q_G \qquad (10)$$

(15) Kubo, R.; Toyozawa, Y. *Prog. Theor. Phys.* **1955**, *13*, 160.
(16) Lin, S. H. *Theor. Chem. Acta* **1968**, *10*, 301.
(17) Kubo, R. *J. Phys. Soc. Jpn.* **1962**, *17*, 1100.
(18) Mukamel, S. *J. Chem. Phys.* **1982**, *77*, 173.
(19) Warshel, A. *Proc. Natl. Acad. Sci. U.S.A.* **1984**, *81*, 444.
(20) Valleau, J. P.; Torrie, G. M. In *Modern Theoretical Chemistry*; Berne, B. J., Ed.; Plenum: New York, Vol. 5, p 137.

where

$$Q_G = \int\int \exp\{-E_G\beta\}\, dS\, dX \quad (11)$$

Multiplying and dividing the numerator by $\exp(-E_G\beta)$ gives

$$Q_m/Q_G = \int\int \exp[-(\epsilon_m - E_G)\beta] \times [\exp(-E_G\beta)/Q_G]\, dS\, dX = \langle \exp\{-(\epsilon_m - E_G)\beta\}\rangle_{E_G} \quad (12)$$

where $\langle\ \rangle_{E_G}$ indicates an average over trajectories that are propagated on E_G. This useful identity is based on the fact that averaging over trajectories of E_G corresponds to integration over the distribution function, $\exp(-E_G\beta)/Q_G$.

It is useful to note that Q_m/Q_G *should not* be evaluated by use of eq 12, because such an approach converges very slowly for large values of $\epsilon_m - E_G$. The real advantage of the umbrella sampling approach can be exploited when Q_m/Q_{m-1} is evaluated for closely spaced X_m and X_{m-1} and then Q_m/Q_G is evaluated by the relation $Q_m/Q_G = (Q_m/Q_{m-1})(Q_{m-1}/Q_{m-2})\cdots(Q_1/Q_G)$. Such an approach converges relatively fast since trajectories on ϵ_{m-1} reach points which contribute significantly to Q_m quite frequently. Note that when the difference between ϵ_m and ϵ_{m-1} is very small we obtain the standard perturbation approach considered in the statistical mechanical textbooks.

While the umbrella sampling method provides a means to evaluate free-energy changes, it does not give a prescription for selecting an effective mapping potential. The selection of the proper potential is not obvious in cases of charge-transfer reactions, where the reaction coordinate involves a concerted polarization of many solvent molecules. Our selection of a mapping potential is based on the idea that the solvent polarization can be mapped most effectively by changing the solute charges. This is done in a convenient way by using a sampling potential of the form

$$\epsilon_m = (1 - \theta_m)\epsilon_1 + \theta_m\epsilon_2 \quad (13)$$

where ϵ_1 and ϵ_2 are the diabatic energies of the reactant and product state, respectively (calculated explicitly for any solvent configuration (**S**) generated by the simulation). The parameter θ_m changes from 0 to 1 upon motion from the reactant to the product region. Using this potential is equivalent in some ways to the charging processes presented in many physics text books, except that it is implemented here on a microscopic level.

The mapping parameter θ can be used as an effective reaction coordinate. Although our selection of the reaction coordinate is quite different (see below), it is instructive to consider the dependence of ΔG_0 on θ_m. This is done in Figure 4 which corresponds to a specific case where $\Delta G_0 = 0$. The figure describes a "charging" process in which we change ϵ_m as a function of θ_m and evaluate the change in free energy associated with changing the charges of the system. Thus, for example, the difference between the maximum and minimum of $\Delta G(\theta)$ gives the difference between the solvation energies of the two benzenes molecules with half electron charge each (held 5 Å apart) and the solvation energy of the benzenes molecules with one electron charge.[31]

After evaluating $\Delta G(\theta_m)$ we are ready for the final step in the evaluation of $q_G(X_m)$. To do this one has to define a unique reaction coordinate. Such a coordinate can be defined in terms of the energy gap by dividing the space of the system into classes, **S**, that satisfy the relationship, $\epsilon_2(S^n) - \epsilon_1(S^n) = C^n$, where C^n is a constant. The locus of point X_n that minimize $\epsilon_1(S^n)$ for positive C^n and $\epsilon_2(S^n)$ for negative C^n can be taken as the reaction coordinate.[8] A somewhat more unique selection is obtained by taking C_n as the reaction coordinate. With this reaction coordinate and the sampling potential of eq 13 we are ready to evaluate the probability function $q_G(X_n)$ of eq 7. That is, the relevant probability factor $q_G(X_n)$ is given by

$$q_G^n = \mathbf{q}_G(X_n)/\mathbf{q}_G(X_a) = (q_m^n/Q_m)(Q_G/q_G^a)(Q_m/Q_G) \times (q_G^n/q_m^n)) = (q_m^n/Q_m)(Q_G/q_G^a)\langle \exp[-(\epsilon_m - E_G)\beta]\rangle_{E_G}(q_G^n/q_m^n) \quad (14)$$

where we use the abbreviation $q_G^n = q_G(X_n)$. The ratio q_m^n/Q_m is evaluated numerically from the ratio between the time a trajectory on ϵ_m is spent between $X_n + \Delta X$ and the total trajectory time. Q_G/q_G^a is evaluated in the same way from a trajectory on E_G. This numerical evaluation converges very fast when the most probable X for ϵ_m is around X_n. The term q_G^n/q_m^n is obtained by

$$q_G^n/q_m^n = \int \exp(-E_G(X_n)\beta)\, dS / \int \exp(-\epsilon_m(X_n)\beta)\, dS = \int \exp[(\epsilon_m - E_G)\beta] \exp(-\epsilon_m\beta)\, dS / \int \exp(-\epsilon_m\beta)\, dS = \langle \exp\{[\epsilon_m(X_n) - E_G(X_n)]\}\rangle_{\epsilon_m} \quad (15)$$

$\epsilon_m(X_n)$ is the value of the sampling potential ϵ_m at X_n.

By knowing what the chance is to be at X_n on the mapping potential ϵ_m, we can calculate the probability to be at X_n on the real ground state potential E_G by means of eq 15. If the off diagonal matrix elements that convert the ϵ_i to E_G are approximately constant for a given X_n, we will have $\epsilon_m(X_n) - E_G(X_n) \simeq$ constant and obtain

$$q_G^n/q_m^n \simeq \exp\{[\epsilon_m(X_n) - E_G(X_n)]\beta\} \quad (16)$$

Now our final expression is

$$\exp(-\Delta g(X_n)\beta) = q_G^n = \exp(-\Delta G_{G\to m}\beta)\langle \exp\{[\epsilon_m(X_n) - E_G(X_n)]\beta\}\rangle_{\epsilon_m}(q_m^n/Q_m)(Q_G/q_G^a) \quad (17)$$

The meaning of this expression can be clarified by an examination of Figure 5. The figure is constructed by taking different sampling potentials (indicated by different symbols) and using them to evaluate by eq 17 the $\Delta g(X_n)$ at the points which occur most frequently with the given potential. For example, in order to evaluate the probability of being at points in phase space where $\Delta\epsilon = -30$ kcal/mol we evaluate the $\Delta G_{G\to m}$ associated with the sampling potential $\epsilon_m = 0.8\epsilon_1 + 0.2\epsilon_2$ and the factor $\langle \exp[\epsilon_m(X)_n - E_G(X_n)]\beta\rangle_{\epsilon_m}$ which converts the probability factor associated with $\Delta G_{G\to m}$ to the one associated with being on E_G at $\Delta\epsilon = -30$ kcal/mol. The factor $(q_m^n/Q_m)(Q_G/q_G^a)$ is close to one and does not change significantly the probability factor. Collecting in this way the $\Delta g(X_n)$ that corresponds to the various $\Delta\epsilon$ gives the free-energy surface for the system.

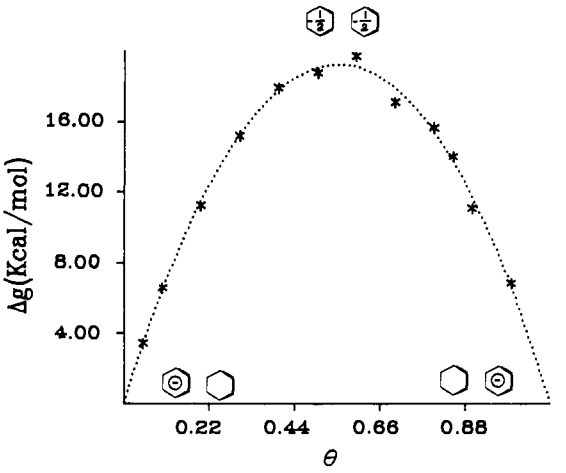

Figure 4. The free energy of the adiabatic charging process for our model system. The figure describes the change of the free energy of the system as a function of the charging parameter θ.

IV. How Quadratic Is the Free Energy Surface?

The approach described above allows one to explore the validity of eq 2 on a microscopic level. This is done here by repeating the same calculations presented in Figure 5 for many values of ΔG_0. Some of these calculations are described in Figure 6. Collecting Δg^* for different values of ΔG_0 gives the results presented in Figure 7. The actual calculations are compared in this figure to the prediction of eq 2 by using the correct microscopic α[14]

$$\alpha = \langle \Delta\epsilon - \Delta G_0\rangle \quad (18)$$

The agreement between the free-energy dependence obtained by the microscopic simulation and the one predicted by eq 2 is

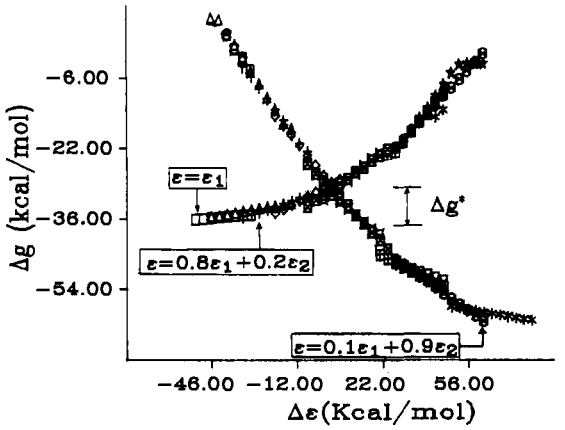

Figure 5. The free-energy profiles of the D^-A and DA^- state as a function of the energy gap. The free energy is calculated by running the trajectories on the different mapping potentials which gradually force the system to change from the initial state to the final state (see the text for details). Different symbols stand for data generated by different mapping potentials, e.g., ⊗, +, and □ for θ_1 = 0.1, 0.8, and 1.0 where $\theta_1 + \theta_2 = 1$.

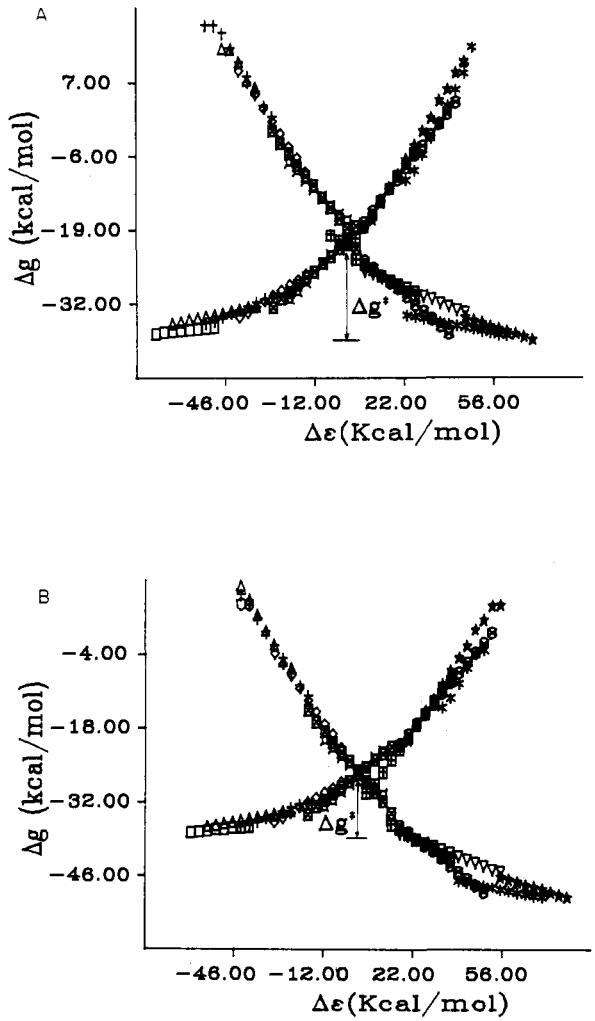

Figure 6. The free-energy profile from ET in our model system for the case when ΔG_0 = 0 kcal/mol and ΔG_0 = −10 kcal/mol.

quite encouraging, considering the fact that the present calculations are subject to convergence error of about 2 kcal/mol. This finding does not mean, however, that the solvent can be described within the harmonic approximation or that the continuum approximation is rigorously valid. In our opinion this result reflects the property of high dielectric solvents which have many equivalent ways for stabilizing charges. Such solvents can give almost the same

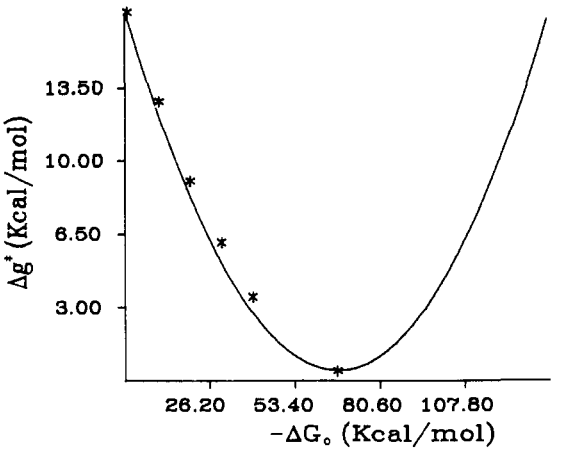

Figure 7. Comparison of the calculated free-energy surface with the one predicted by Marcus' relationship. The calculations were obtained by repeating the calculations described in Figures 5 and 6 and obtained Δg^* as a function of ΔG_0.

solvation energies by either large anharmonic deformation of few solvent molecules near the solute or small harmonic motions of many molecules far from the solute.[24] Since both type of free-energy contributions are similar in magnitude, it will require more studies and careful analysis to decide whether the actual contributions of the solvent are associated with harmonic or anharmonic polarization of the solvent.

It should be pointed out that the actual value of α is not given in a quantitative way by the macroscopic theory since the effective cavity radius is not defined uniquely.[30] For example, our calculated α is about 32 kcal/mol. This value should have been about 16 kcal/mol if the induced dipoles of the system were included in the simulation. On the other hand, the macroscopic estimate[1] with a reasonable cavity radius of 4 Å for the benzene molecule is 8 kcal/mol. A very different result is obtained if the effective cavity radius is determined consistently by following ref 29 and fitting the calculated solvation energy to the Born's model. This gives a radius of 2.37 Å (for solvation of −70 kcal/mol) and an α value (from $\alpha = 166(1/a - 1/R)$ of $\simeq$ 37 kcal/mol. Similar problems were reported in Figure 6 of ref 7.

V. The Deviations from Marcus' Relationship Are Associated with Vibronic Channels

As indicated from the previous section one can approximate the solvent contribution to the activation barrier by a quadratic

(21) Warshel, A.; Sussman, F. *Proc. Natl. Acad. Sci. U.S.A.* **1986**, *83*, 3806.
(22) Warshel, A.; King, G. *Chem. Phys. Lett.* **1985**, *121*, 124.
(23) Warshel, A. *Proc. Natl. Acad. Sci. U.S.A.* **1980**, *77*, 3105.
(24) Experimentally one finds that ions are stabilized in the gas phase by small cluster of water molecules as much as they are solvented in aqueous solutions.[25] However, in aqueous solutions the bulk solvent gives a significant part of the total solvation energy.
(25) Kebarle, P. A. *Rev. Phys. Chem.* **1977**, *28*, 445.
(26) (a) Warshel, A. In *Modern Theoretical Chemistry*; Segal, G., Ed.; Plenum Press: New York, 1977; Vol. 7. (b) Warshel, A.; Levitt, M. Indiana University, *QCPE* **1974**, No. *247*.
(27) An interesting attempt[28] to evaluate reorganization energy experimentally is based on the assumption that observed threshold energy for electron emission includes the energy of the unrelaxed solvent. However the threshold energy should be somewhat below the energy of the unrelaxed excited state due to the solvent Franck–Condon factors. Furthermore, such experiments are not available for donor and acceptor at a finite separation.
(28) (a) Delahay, P.; Dziedzic, A. *J. Chem. Phys.* **1984**, *11*, 5381. (b) Delahay, P.; Dziedzic, A. *Ibid.* **1984**, *11*, 5793.
(29) Warshel, A. *Israel J. Chem.* **1981**, *21*, 341.
(30) Warshel, A.; Russell, S. T. *Quart. Rev. Biophys.* **1984**, *17*, 283.
(31) Our independent estimate of the solvation of a benzene ion is around −70 kcal/mol. This can be used to examine $\Delta G(\theta)$ by calculating the difference $\Delta\Delta G = \Delta G(^1/_2) - \Delta G(0)$ where $\Delta G(0)$ is equal to the solvation of a benzene ion, and $\Delta G(^1/_2)$ can be determined by the powerful relationship (page 335 of ref 30), $\Delta G_{sol}(R) = \Delta G_{sol}(\infty) - 332 q_1 q_2/R$, where $\Delta G_{sol}(\infty)$ is the solvation energy of two benzene ions each with a charge of $^1/_2$. With $\Delta G_{sol}(\infty)$ = −35 kcal/mol one obtains $\Delta G(^1/_2)$ = −52 kcal/mol which gives $\Delta\Delta G$ = 18 kcal/mol, in good agreement with our direct calculations.

Table II.

frequencies	0–1	0–2	0–3	0–4	0–5
The Franck–Condon Factors of Reducing Quinone[a]					
1699	1.2252	0.8052	0.3758	0.1394	0.0436
1491	0.0390	0.011			
1120	0.0783	0.0075			
467	0.9284	0.4727	0.1739	0.0515	0.0130
The Franck–Condon Factors of Oxidizing Biphenyl[a]					
1660	0.4612	0.1275	0.0270	0.0048	
1518	0.0365	0.0032			
1369	0.0634	0.0057			
1002	0.0906	0.0090			
775	0.0427	0.0037			
351	0.1114	0.0121	0.0011		

[a] Frequencies in cm^{-1}, Franck–Condon factors in dimensionless units. The reported values were obtained by QCFF/PI method.

function. Yet experimental studies of the dependence of $\Delta g^{\ddagger}$ on ΔG_0 seem to give very large deviations from eq 2 at the so called "inverted region" where $|\Delta G_0| > \alpha$. The origin of this deviation can be best understood by applying our semiclassical approach to transitions between vibronic levels, rather than electronic levels. This gives

$$C_{am,bm'}(\tau) = \int_0^{\tau} -(i/\hbar)S_{m,m'}\sigma \exp\left\{(i/\hbar)\int_0^t dt'\Delta\epsilon_{am,bm'}(r(t'))\right\} dt$$

where the $\Delta\epsilon$ is given by

$$\Delta\epsilon_{bm',am} = (\epsilon_b - \epsilon_a) + \hbar\sum_r \omega_r(m'_r - m_r) \qquad (19)$$

Here ω_r is the internal frequency of the solutes, and $S_{mm'}$ is the Franck–Condon factor for the vibronic transition between states.

The effective activation free energy associated with eq 19 can be written as[14]

$$\Delta g^{\ddagger}_{mm'} = [\Delta G_0 - \sum_r \hbar\omega_r(m'_r - m_r) + \alpha]^2/4\alpha - RT \ln (S_{mm'}) \qquad (20)$$

The experimental examination of the validity of eq 20 cannot be accomplished without a clear idea about the Franck–Condon factors $S_{mm'}$. This can be done by the QCFF/PI approach[26] which allows one to calculate directly the Franck–Condon factors associated with different electronic transitions (including ET processes) in conjugated molecules.

For example, we evaluate here the Franck–Condon factors associated with the oxidation of biphenyl and the reduction of quinone, which are typical components of the molecules used in the experiments of ref 9. The corresponding Franck–Condon factors listed in Table II and a solvent reorganization energy of 0.8 eV give the result presented in Figure 8. This result which reproduces the observed experimental trend is not brought here as an analysis of the experimental series (this should be done by calculating the reorganization energy for each donor and acceptor) but for demonstration that the deviations from eq 2 are due to vibronic channels.

The idea that vibronic channels may be important in the inverted region is not new.[3c,23,9a] However, the question addressed here is not what are the possible explanations for the deviations from Marcus's relationship, but what are the actual reasons. We believe that the answer for this question cannot be determined without explicit evaluation of the relevant molecular Franck–Condon factors.

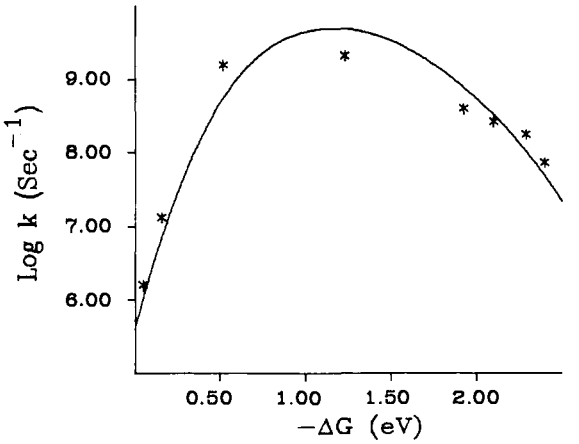

Figure 8. Showing the effect of intramolecular vibronic channels on the rate constant. The figure uses eq 20 with the calculated Franck–Condon factors of Table I for a biphenyl + quinone system. The σ used is estimated from ref 9. The result is quite similar to those obtained in the experimental study of ref 9 (denoted by *).

VI. Concluding Remark

This paper explores the free-energy relationship for ET reactions by using microscopic simulation approach. The adiabatic charging method appears to give converging results, indicating that it can be used in exploring the solvent contribution in series of donors and acceptors. The model system used here (the benzene + water system) gives free-energy surface which follows to a good approximation the Marcus' relationship. This type of quadratic relationship is associated with the contribution of the solvent to the activation barrier (or to the barrier expected when the solute does not change its geometry upon ET). In realistic experimental systems the solute undergoes significant geometry changes, and the observed barrier at the inverted region is much smaller than that predicted by eq 2. The reason for this, as demonstrated in the previous section, is the availablility of vibronic channels which eliminates the need to overcome the complete solvent barrier.

The agreement between the simulated free-energy curve and eq 2 might give the impression that polar solvents can be described reliably by the quadratic approximation or by the linear response theory. This agreement might be accidental in the following sense: The reorganization energy associated with polarizing the first solvation shells might be similar to that obtained by small displacement of many water molecules in distant solvation shells. Thus, while in reality the solvent polarization might correspond to the anharmonic saturation limit, the observed results might be similar to those expected from harmonic solvents. If, however, the actual reorganization energy is due to the harmonic polarization of the solvent, then the microscopic basis of macroscopic dielectric theories might be more valid than previously suspected.

Acknowledgment. This work was supported in part by Grant No. PCM-8303385 from the National Science Foundation.